A TWO-PHASE GENETIC ALGORITHM TO MODEL THE MENISCAL HORN REPAIRED WITH SUTURE

Estebanez B. (1), Peña-Trabalón A. (1), Moreno-Vegas S. (1), Espejo-Reina A. (1, 2), Nadal F. (1), García-Vacas F. (1), Perez-Blanca A. (1), Prado-Novoa M. (1)

1. *Clinical Biomechanics Laboratory of Andalusia, University of Malaga, Spain*
2. *Vithas Malaga Hospital, Spain*

Introduction

Menisci suturing is a common surgical technique nowadays. Menisci have been modeled with different degrees of complexity in finite element models (FEM) of the human knee [1], but there are few works focused on simulating the meniscus subjected to traction loads in its longitudinal direction [2], such as those produced by sutures after repair. Moreover, there are no models that include the effect of the orifice for the suture. This study develops a material model of the meniscal horn when it is pulled by the thread used to reattach its root.

Methods

For the experimental data, the anterior horn of a human medial meniscus pierced by a Nº2 suture was used. Its surface was marked with 4 ink dots, 2 at the thread insertion and 2 far from this area. A displacement-controlled load-to-failure test was performed on a uniaxial testing bench, as shown in Figure 1a, with the traction load aligned with the meniscal fibers and with the suture. The displacements of the dots were recorded by a videogrammetric system synchronized with the machine load cell, which computed the distances between the ink marks as a function of the traction force until the beginning of the tissue cut-out.

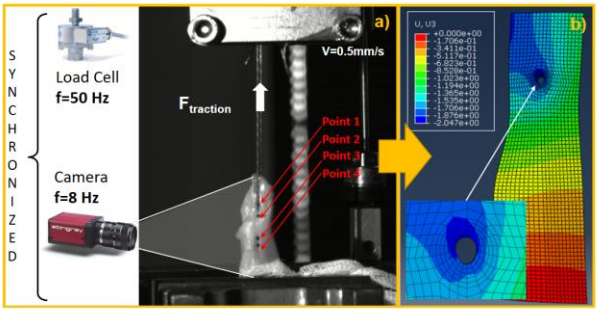

Figure 1: Specimen on the testing bench and its model.

A FEM of the meniscal horn reproducing the boundary and load conditions of the test was developed in Abaqus (Figure 1b). Hyperelastic incompressible Mooney-Rivlin models of 2 and 3 parameters [3] were used for the tissue. To identify the model parameters, a two-phase genetic algorithm was developed. In the first phase, the engineering stress (σ) was computed as a function of the experimental strain ratio (λ) assuming homogenous isotropic material, thus disregarding the orifice, and uniaxial traction [3]:

$$\sigma^{theo} = 2C_{10}(\lambda - \lambda^{-1}) + 2C_{01}(1 - \lambda^{-3}) + 6C_{11}(\lambda^2 - \lambda - 1 + \lambda^{-2} + \lambda^{-3} - \lambda^{-4}) \quad (1)$$

While the experimental stress was estimated as:

$$\sigma^{exp} = F/A \quad (2)$$

F being the measure traction force and A the initial meniscal cross-section at the suture point. The parameter set, $\{C_{10}, C_{01}\}$ for the 2-parameter model or $\{C_{10}, C_{01}, C_{11}\}$ for the 3-parameter model, were found minimizing the RMS between σ^{theo} and σ^{exp} searching in a wide domain ($\pm 10^6$ MPa for all parameters). In the second phase, the model parameters were recomputed by minimizing the RMS between λ^{exp}, the strain ratio experimentally measured in the orifice area, and λ^{theo}, the value simulated for the same points by the FEM of the meniscus. For this phase, with a much higher computational cost, the parameters of the first phase acted as seeds narrowing the search domain around them (first phase results ±5 MPa for all parameters).

Results and Discussion

The model parameters found by each phase of the material optimization algorithm are shown in Table 1 for the 2- and 3- parameter Mooney-Rivlin models, respectively. The computational time and RMS in the orifice area achieved by each phase are also detailed. The 3-parameter model was more suitable to simulate the strain near the meniscal orifice. However, the RMS for the marks far from the orifice was greater than 0.01, suggesting that a different material model is needed for each tissue area. Not including the first optimization phase was checked with a relatively small initial domain (±500MPa for all parameters), but after 12 hours the RMS still made it unfeasible.

Phase	C_{01}	C_{10}	C_{11}	RMS	Time
Mooney-Rivlin model of 2 parameters					
1	1.8450	-0.9801	-	0.00016	1.0s
2	0.6131	-0.0948	-	0.0204	4.8h
Mooney-Rivlin model of 3 parameters					
1	1.7468	-0.8775	0.0892	0.00018	0.8s
2	2.2866	-1.8706	1.3968	0.00012	6.8h

Table 1: Material optimization results.

References

1. Seyfi B. et al, J Mech B of Biomed Mat, 77: 337-346, 2018.
2. Abraham A. C. et al, J Biomech, 44:413-418, 2011.
3. Kumar N. et al, MIT Int J of Mech Eng, 6:43-46, 2016.

Acknowledgements

This work was supported by the Spanish Government (grant RTI2018-094339-B-I00), Junta de Andalucía (grant P20-00294) and the University of Malaga.